

B. B. Dumre, R. J. Ellingson, S. V. Khare, Solar Energy Materials and Solar Cells 248, 111971, Supplementary Material (2022)

Effects of short-range order in phase equilibria and opto-electronic properties of ternary alloy $Zn_xCd_{1-x}Te$

B. B. Dumre^a, R. J. Ellingson^a, S. V. Khare^{a,*}

^aDepartment of Physics and Astronomy, and Wright Center for Photovoltaics Innovation and Commercialization

(PVIC), University of Toledo, Toledo, OH 43606, USA

*Corresponding Author: bishalbabu.dumre@rockets.utoledo.edu

Supplementary Material

B. B. Dumre, R. J. Ellingson, S. V. Khare, Solar Energy Materials and Solar Cells 248, 111971, Supplementary Material (2022)

Table S1: Equilibrium lattice parameters and formation energies of $Zn_xCd_{1-x}Te$ alloys per formula unit in B3 crystal structure, computed using GGA functional. Values from the literature are listed where

Material	Lattice Constant a (\AA)	Volume V (\AA^3)	Formation Energy (eV)
CdTe	6.62, 6.48 ^a , 6.54 ^b	290.12	- 0.96
$Zn_{0.25}Cd_{0.75}Te$	6.52	277.17	- 0.95
$Zn_{0.50}Cd_{0.50}Te$	6.42, 6.365 ^c	264.61	- 0.95
$Zn_{0.75}Cd_{0.25}Te$	6.30	250.05	- 0.95
ZnTe	6.18, 6.08 ^d , 6.1026 ^e	236.03	- 0.97

available.

^aTheoretical Ref. [1]

^bExperimental Ref. [2]

^cExperimental Ref. [3]

^dTheoretical Ref. [4]

^eExperimental Ref. [5]

Table S2: Electronic band gaps of $Zn_xCd_{1-x}Te$ alloys, calculated implementing GGA and hybrid HSEO6 functionals. Values from the literature are listed where available.

Material	Band Gap, Direct (eV)		
	GGA	HSEO6	Other Works
CdTe	0.94	1.54	1.31 ^a , 1.50 ^b
$Zn_{0.25}Cd_{0.75}Te$	0.99	1.49	-
$Zn_{0.50}Cd_{0.50}Te$	1.05	1.60	-
$Zn_{0.75}Cd_{0.25}Te$	1.15	1.77	-
ZnTe	1.28	2.39	2.24 ^{c,d} , 2.39 ^{e,f}

^aTheoretical (FPLAW, EV-GGA) Ref. [6]

^bExperimental Ref. [7]

^cTheoretical (LDA) Ref. [1]

^dExperimental Ref. [8]

^eExperimental Ref. [9]

^fExperimental Ref. [10]

Table S3: Average and standard deviation of band structure effective masses (m^*) of electrons and holes of $Zn_xCd_{1-x}Te$ alloys. Values are given in units of electron mass (m_o).

Material	Electron Effective Mass (m_e^*)		Hole Effective Mass (m_h^*)	
	Average	Standard Deviation	Average	Standard Deviation
CdTe	1.33	1.01	0.17	0.10
$Zn_{0.25}Cd_{0.75}Te$	1.56	0.88	0.35	0.26
$Zn_{0.50}Cd_{0.50}Te$	1.74	1.05	0.37	0.28
$Zn_{0.75}Cd_{0.25}Te$	1.53	0.94	0.40	0.32
ZnTe	1.20	0.94	0.17	0.10

Table S4: Charge transfer from Cd and Zn to Te in $Zn_xCd_{1-x}Te$ alloys computed using the Bader charge segregation scheme [11-14]. Values are given in elementary charge units.

Material	Cd	Zn
CdTe	0.52	N/A
$Zn_{0.25}Cd_{0.75}Te$	0.51	0.52
$Zn_{0.50}Cd_{0.50}Te$	0.51	0.52
$Zn_{0.75}Cd_{0.25}Te$	0.50	0.51
ZnTe	N/A	0.50

Table S5: Dielectric constants of $Zn_xCd_{1-x}Te$ alloys calculated using the hybrid HSE06 functional.

Material	Dielectric Constant
CdTe	5.87
$Zn_{0.25}Cd_{0.75}Te$	6.36
$Zn_{0.50}Cd_{0.50}Te$	6.45
$Zn_{0.75}Cd_{0.25}Te$	6.53
ZnTe	6.04

Table S6: Charge carrier mobility, Urbach Energy, and Exciton Binding Energy of $Zn_xCd_{1-x}Te$ alloys calculated using the hybrid HSEO6 functional.

Material	Hole Mobility (cm ² /Vs)	Electron Mobility (cm ² /Vs)	Urbach Energy (meV)	Exciton Binding Energy (meV)
CdTe	103.42, 100 ^a	13.21	18.94, 15 ^c	45.01
$Zn_{0.25}Cd_{0.75}Te$	50.23	11.27	21.97	96.46
$Zn_{0.50}Cd_{0.50}Te$	47.52	10.10	20.72	97.86
$Zn_{0.75}Cd_{0.25}Te$	43.95	11.49	21.17	83.09
ZnTe	103.42, 100 ^b	14.65	23.08	91.62

^aExperimental Ref. [15] (At 225 K temperature)

^bExperimental Ref. [16] (At 275 K temperature)

^cExperimental Ref. [17]

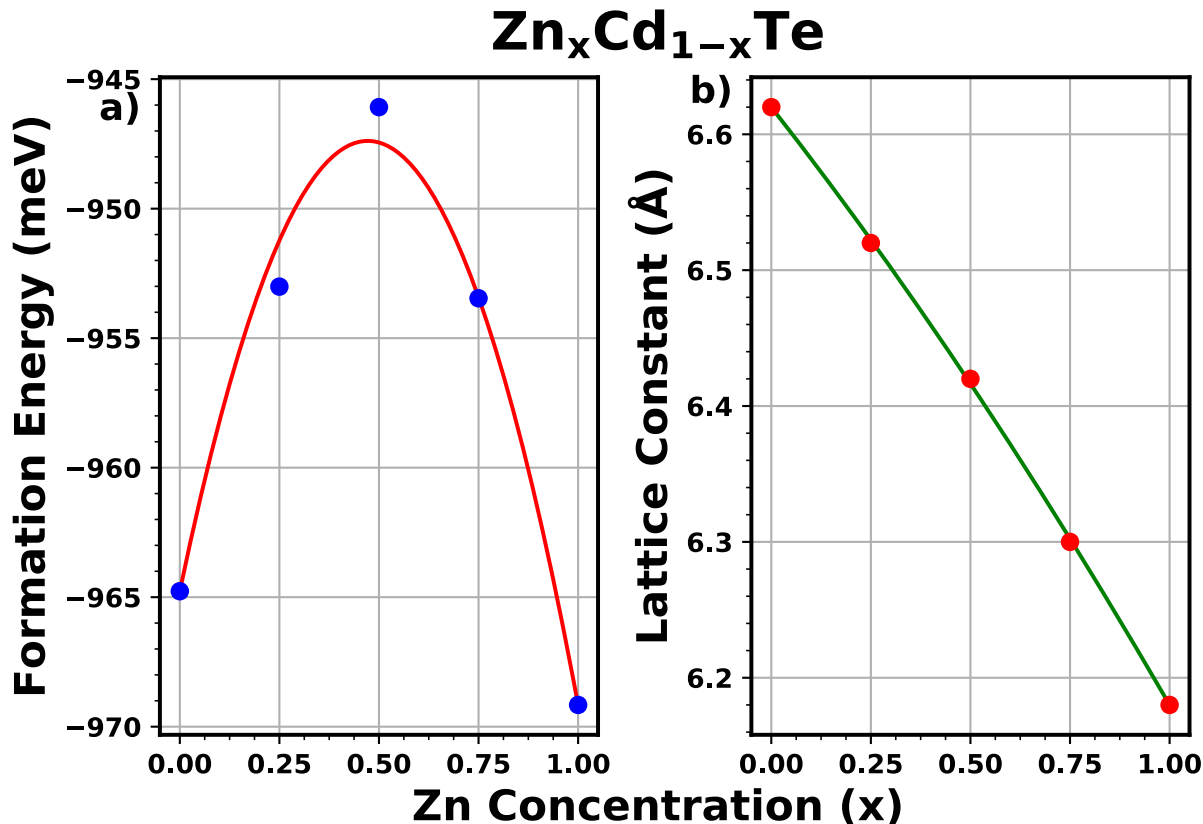


Figure S1: a) Formation energies, and b) lattice constants of Zn_xCd_{1-x}Te alloys calculated using the GGA functional. Here, points denote calculated values whereas curves sketch fitting based on a bowing parameter defined in Eq. (3).

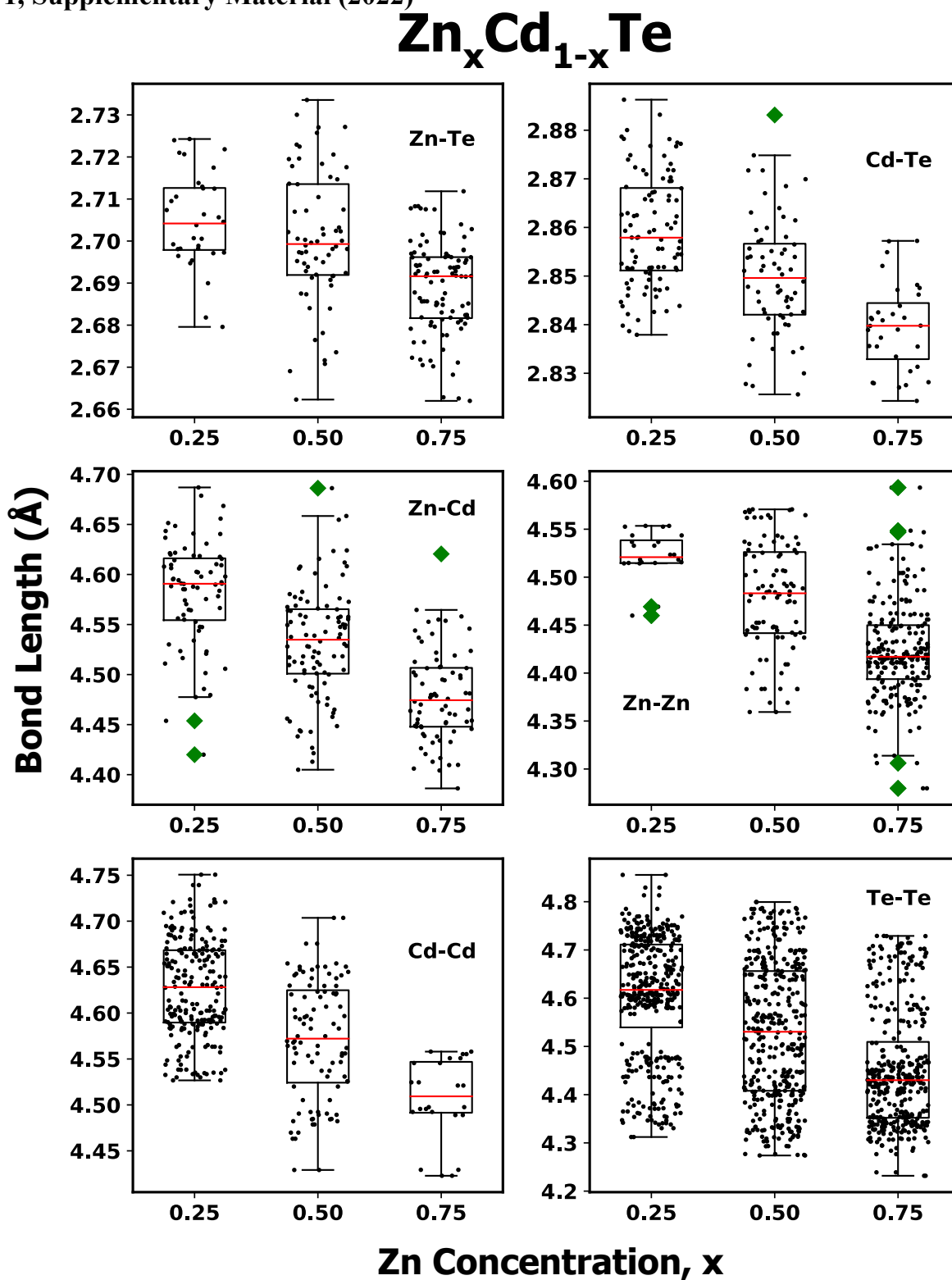


Figure S2: Box-and-whisker plots displaying the distribution of various first nearest neighbor bond lengths (Zn-Te, Cd-Te, Zn-Cd, Zn-Zn, Cd-Cd and Te-Te) at intermediate Zn concentrations ($x = 0.25, 0.50, 0.75$) within disordered Zn_xCd_{1-x}Te alloys, simulated using SQS. Horizontal red lines denote the median whereas the green diamonds denote the outliers.

$Zn_xCd_{1-x}Te$

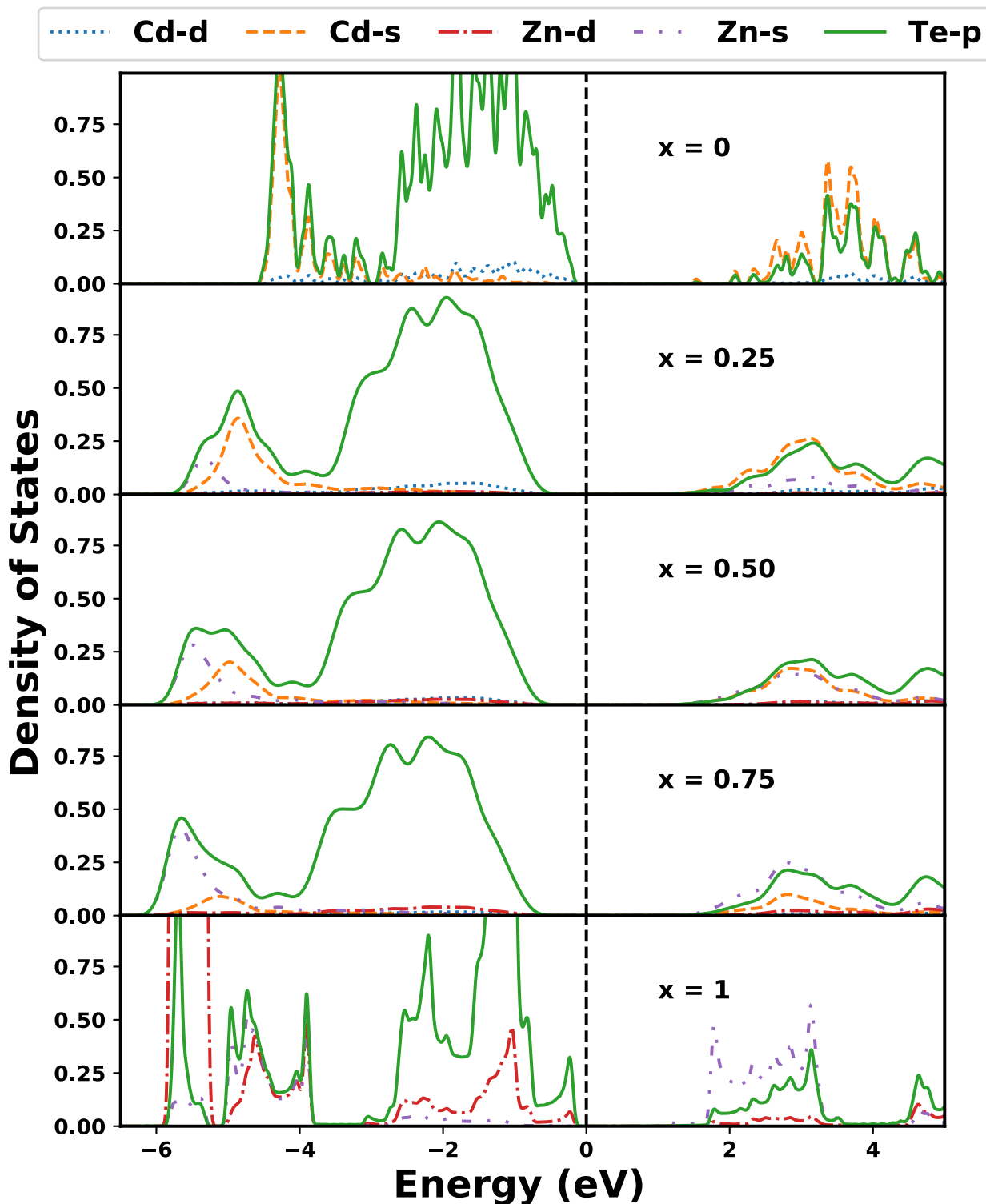


Fig S3: On-site projected electronic density of states (PDOS) per formula unit of $Zn_xCd_{1-x}Te$ alloys calculated using the HSE06 functional. The Fermi level is set to 0 eV.

$Zn_xCd_{1-x}Te$

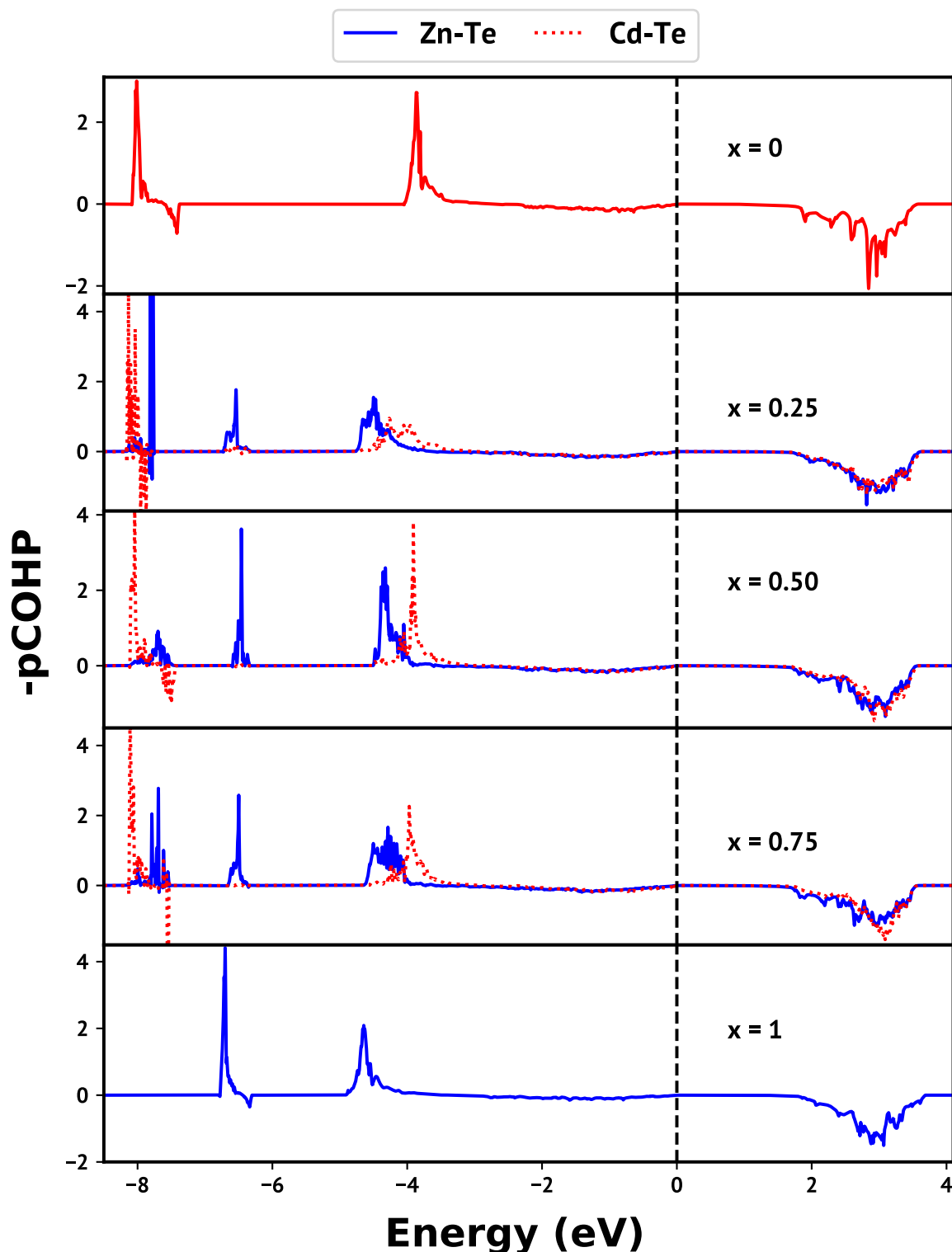


Figure S4: Projected Crystal Orbital Hamiltonian Populations (-pCOHP) of nearest-neighbors' interactions of $Zn_xCd_{1-x}Te$ alloys. All other covalent interactions are negligible compared to Cd-Te and

Zn-Te pairs displayed here. Positive and negative values of -pCOHP correspond to bonding and antibonding interactions respectively. The Fermi level is set to 0 eV.

$Zn_xCd_{1-x}Te$

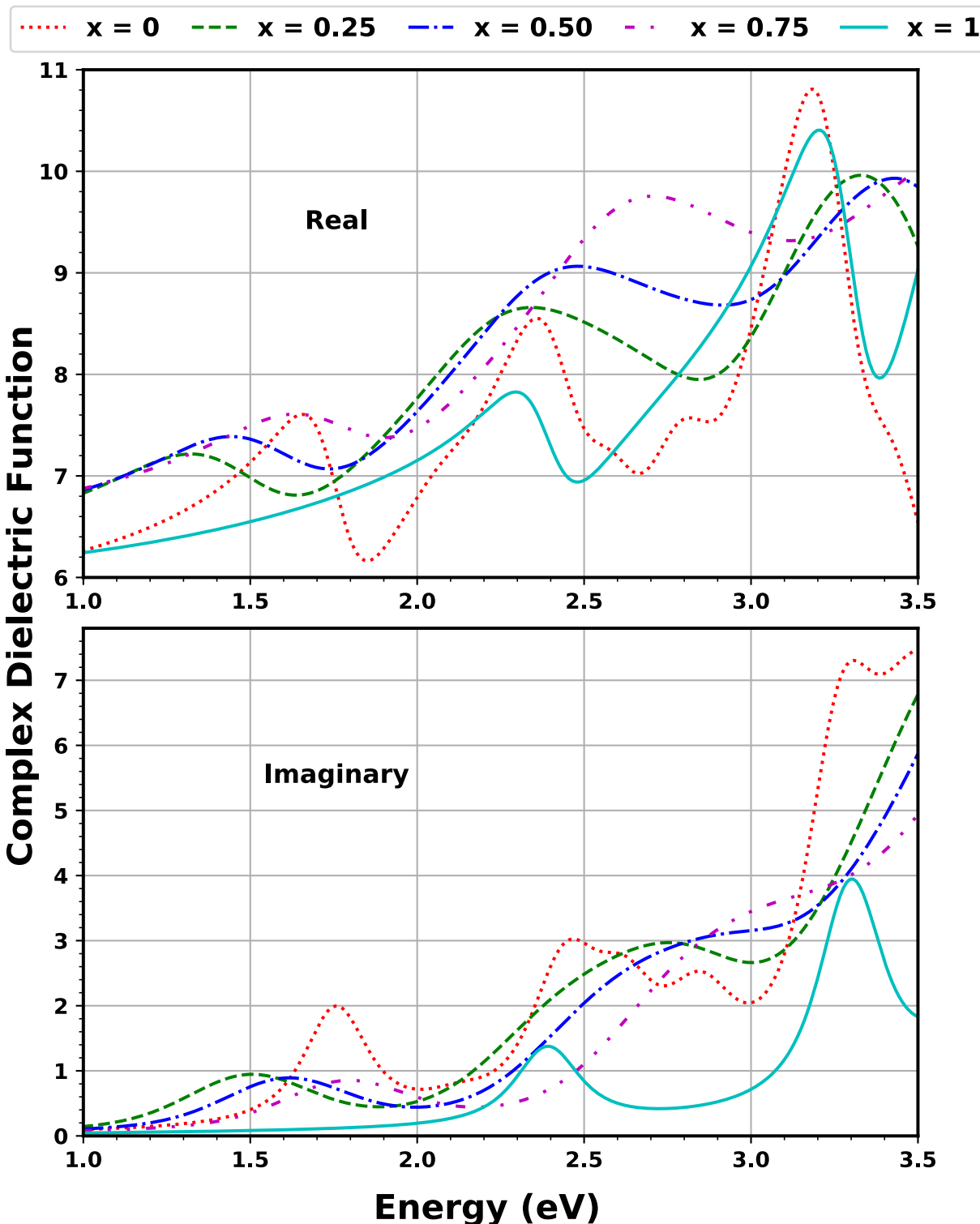
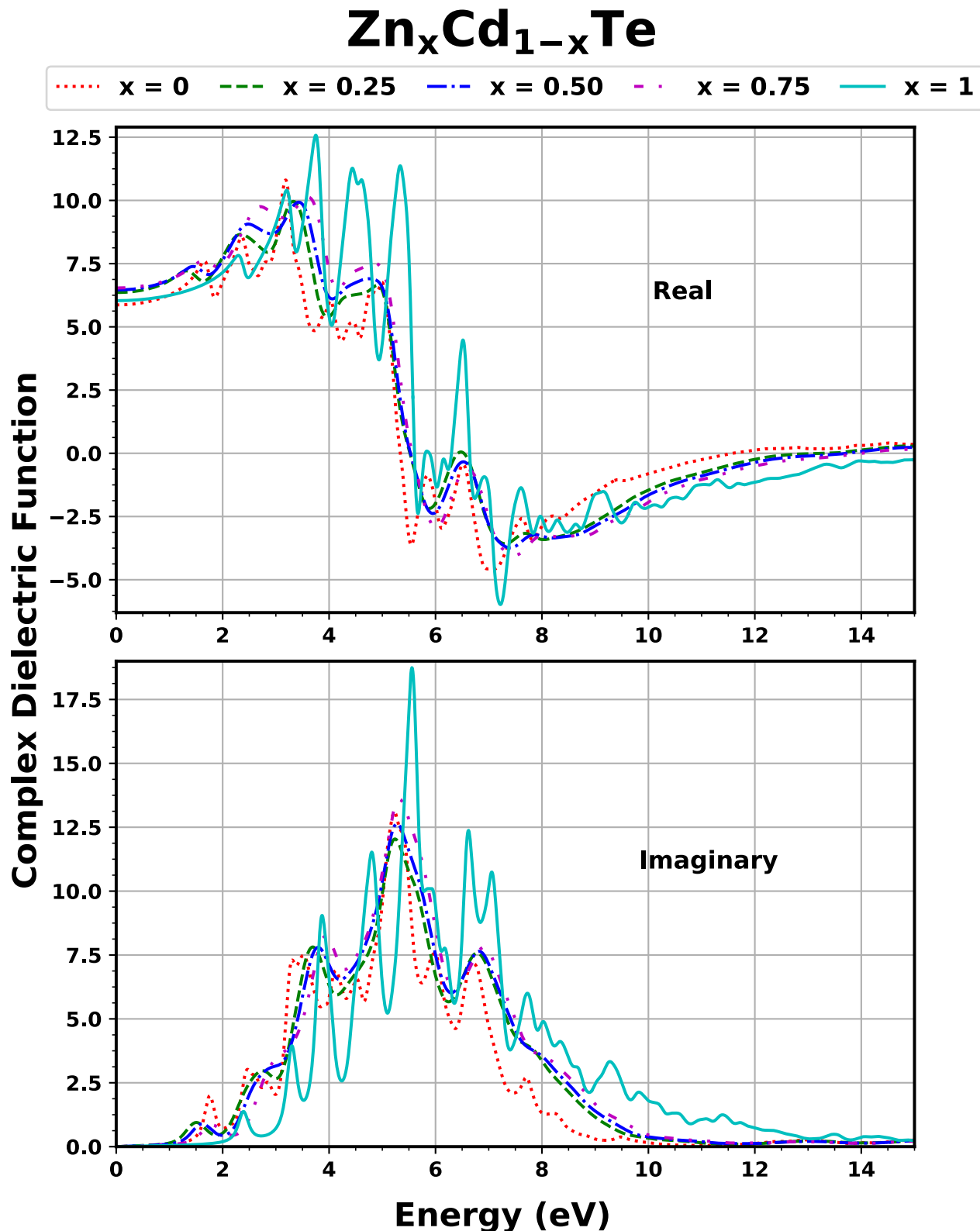


Figure S5: Complex dielectric functions of $Zn_xCd_{1-x}Te$ alloys computed utilizing the hybrid HSE06 functional. Photon energies shown are in the visible-UV range.



B. B. Dumre, R. J. Ellingson, S. V. Khare, Solar Energy Materials and Solar Cells 248, 111971, Supplementary Material (2022)

Figure S6: Variation of complex dielectric functions of $Zn_xCd_{1-x}Te$ alloys, calculated using the hybrid HSEO6 functional. Photon energies shown are in the range (0-15) eV.

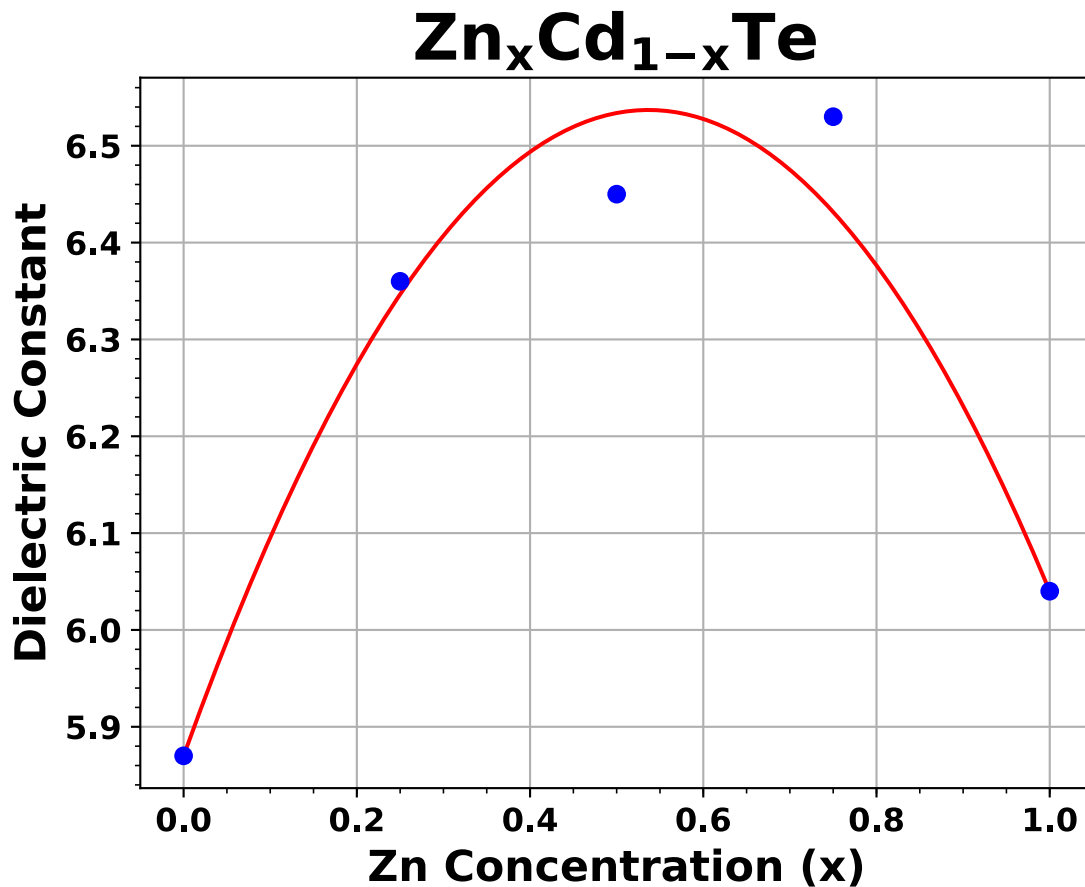


Figure S7: Dielectric constants of Zn_xCd_{1-x}Te alloys calculated using the hybrid HSEO6 functional. Here, points denote calculated values whereas curves sketch fitting based on a bowing parameter defined in Eq. (3).

References:

1. Huang, M.-Z. and W.Y. Ching, *Calculation of optical excitations in cubic semiconductors. I. Electronic structure and linear response*. Physical Review B, 1993. **47**(15): p. 9449-9463.
2. Mangalhara, J.P., R. Thangaraj, and O.P. Agnihotri, *STRUCTURAL, OPTICAL AND PHOTOLUMINESCENCE PROPERTIES OF ELECTRON BEAM EVAPORATED CdSe_{1-x}Te_x FILMS*. Solar energy materials, 1989. **19**(3-5): p. 157-165.
3. Wang, Y., et al., *Synthesis and optical properties of composition-tunable and water-soluble Zn_xCd_{1-x}Te alloyed nanocrystals*. Journal of Crystal Growth, 2007. **308**(1): p. 19-25.
4. Korozlu, N., K. Colakoglu, and E. Deligoz, *Structural, electronic, elastic and optical properties of Cd_xZn_{1-x}Te mixed crystals*. Journal of Physics: Condensed Matter, 2009. **21**(17): p. 175406.
5. Wu, Y., et al., *Growth of Cd_{1-x}Zn_xTe thin films with high Zn content by close-spaced sublimation*. Vacuum, 2016. **132**: p. 106-110.
6. Reshak, A.H., et al., *Effect of increasing tellurium content on the electronic and optical properties of cadmium selenide telluride alloys CdSe_{1-x}Te_x: An ab initio study*. Journal of Alloys and Compounds, 2011. **509**(24): p. 6737-6750.
7. Compaan, A.D., et al., *PROPERTIES OF PULSED LASER DEPOSITED CdS_xTe_{1-x} FILMS ON GLASS*. MRS Proceedings, 1996. **426**: p. 367.
8. Oklobia, O., G. Kartopu, and S.J.C. Irvine, *Properties of Arsenic-Doped ZnTe Thin Films as a Back Contact for CdTe Solar Cells*. Materials, 2019. **12**(22): p. 3706.
9. Harrison, W.A., *ELECTRONIC STRUCTURE AND THE PROPERTIES OF SOLIDS: The Physics of the Chemical Bond*. 2012: Courier Corporation.
10. Noda, D., et al., *Zn_xCd_{1-x}Te Epitaxial Growth by Remote Plasma Enhanced MOCVD Method*. MRS Online Proceedings Library, 1997. **487**(1): p. 45-49.
11. Henkelman, G., A. Arnaldsson, and H. Jónsson, *A fast and robust algorithm for Bader decomposition of charge density*. Computational Materials Science, 2006. **36**(3): p. 354-360.
12. Sanville, E., et al., *Improved grid-based algorithm for Bader charge allocation*. Journal of Computational Chemistry, 2007. **28**(5): p. 899-908.
13. Tang, W., E. Sanville, and G. Henkelman, *A grid-based Bader analysis algorithm without lattice bias*. Journal of Physics: Condensed Matter, 2009. **21**(8): p. 084204.
14. Yu, M. and D.R. Trinkle, *Accurate and efficient algorithm for Bader charge integration*. The Journal of Chemical Physics, 2011. **134**(6): p. 064111.
15. Turkevych, I., et al., *High-temperature electron and hole mobility in CdTe*. Semiconductor Science and Technology, 2002. **17**(10): p. 1064-1066.
16. Aven, M. and B. Segall, *Carrier Mobility and Shallow Impurity States in ZnSe and ZnTe*. Physical Review, 1963. **130**(1): p. 81-91.
17. Chantana, J., et al., *Impact of Urbach energy on open-circuit voltage deficit of thin-film solar cells*. Solar Energy Materials and Solar Cells, 2020. **210**: p. 110502.